Supporting Information for:

Dehydrogenation of dimethylamine-borane mediated by Group 1 pincer complexes

Roberto Nolla-Saltiel, Ana M. Geer, William Lewis, Alexander J. Blake and Deborah L. Kays*[a]

[a]School of Chemistry, University of Nottingham, University Park, Nottingham,

NG7 2RD, United Kingdom.

Table of Contents

General Procedures

Synthesis of Compounds

- Synthesis of 1
- Synthesis of 2
- Synthesis of 3
- Synthesis of 4

General Experimental Procedures

NMR spectra of Compounds

DOSY NMR Studies

X-ray crystallography

References

General Procedures

Apart from the synthesis of the ligand, all products described were treated with rigorous exclusion of air and water using standard air-sensitive-handling techniques which included bench-top operations (Schlenk line) and glove-box techniques. Standard laboratory solvents were pre-dried putting them in contact with meticulous drying and deoxygenating agents such as sodium wire and subsequently dried *via* reflux over potassium (toluene) or sodium-benzophenone ketyl (tetrahydrofuran). d_6-benzene was dried over potassium in a sealed ampoule at 80 °C for 4 days, before vacuum-transferring it to an ampoule containing a potassium mirror and subsequently stored in the glovebox prior to use. NMR samples of air and moisture sensitive compounds were prepared using glove box techniques and contained in Young´s tap modified borosilicate glass NMR tubes. All NMR data was collected on Bruker DPX300, DPX400, AV400, AV(III)400, AV(III)400HD or AV(III)600 spectrometers. Chemical shifts are quoted in ppm relative to TMS (^{1}H, ^{13}C), LiCl/D_2O solution (^{7}Li{^{1}H}) and $BF_3 \cdot OEt_2$ (^{11}B, ^{11}B{^{1}H}). DOSY experiments were carried out using the PFGSE (Pulsed-Field Gradient Spin-Echo) NMR Diffusion methods and analysed with the software implemented by Bruker on an AV(III)600 NMR spectrometer. The variation of the intensity (integral) of one selected signal in the ^{1}H NMR spectrum (I) is related to the strength of the gradient (G) by the following equation: $Ln(I/Io) = - \gamma^2 \delta^2 Gi^2 (\Delta-\delta/3) D$, where γ = gyromagnetic ratio of the proton, δ = length of the gradient pulse, Gi = gradient strength, Δ = delay between the midpoints of the gradients, and D = diffusion coefficient. Before recording the DOSY experiment, the values of δ (small delta) and Δ (big delta) were optimized for each complex. The selected values provided a considerable reduction of the intensity of the signal, but it remained strong enough to be integrated. Next, the bidimensional DOSY experiment (stebpgp1s sequence) was recorded with the optimized δ and Δ values, varying G along 16-32 spectra. The data were analysed with the Bruker's software, which provided directly the diffusion coefficient (D). The quality of the data was tested by representation Ln(I) versus G2, which gave an excellent fit to a straight line in all the cases. Hydrodynamic radii (r_H) were calculated from the Stokes–Einstein equation: $r_H = (k*T)/(6*\pi*\eta*D)$ (where T is absolute temperature, k is the Boltzmann constant, η is the solvent viscosity and D is the coefficient of diffusion). Averaged molecular radii were estimated from the calculated molecular volume defined as the volume inside a contour of 0.001 electrons/Bohr^3. Air-sensitive mass spectrometry samples were prepared under an argon atmosphere by placing the sample inside glass capillaries. The spectra for the complexes described were recorded by the EPSRC National Mass Spectrometry Facility at Swansea University. Non air-sensitive samples were prepared by careful dilution of the sample in methanol and run through the departmental service at the School of Chemistry, University of

Nottingham using a Bruker MicroToF (ESI+/ESI-). Air sensitive infrared spectroscopy samples were prepared as Nujol mulls between two KBr discs, while non air-sensitive samples were recorded (ATR) using a Bruker ALPHA FTIR spectrometer over a frequency range of 4000-400 cm^{-1}. UV/vis spectroscopy samples were prepared as solutions of known concentration in a Young's tap modified 10 mm quartz cell. UV/vis spectra were recorded on a Perkin Elmer Lambda 750 UV/vis spectrophotometer, over a wavelength range of 350-1100 nm. $Me_2NH \cdot BH_3$ and $Me_3N \cdot BH_3$ were purchased from Sigma-Aldrich and used as received. ^tBuLi was purchased from Sigma-Aldrich as a 1.7 M solution in pentane, the solution was transferred to a Schlenk flask and the volatiles were removed under vacuum, affording a light-yellow powder which was stored in the glovebox. NaH and KH were washed with hexane and filtered, the resulting filtrate was dried under vacuum and transferred to the glovebox, prior to use. **Safety warning:** 1-Naphthylamine is highly toxic and is suspected to be a carcinogen; great care must be taken during synthesis and adequate handling of waste should be procured. **Safety warning:** Dehydrocoupling of $Me_2NH \cdot BH_3$ with precatalysts **2-4** evolves $H_2(g)$.

Synthesis of 1,8-dinaphthylimino-3,6-di(^tButyl)-9H-carbazole (**1**):

1,8-diformy-3,6-di(^tButyl)-9H-carbazole (2 g, 5.9 mmol), 1-Naphthylamine (1.7 g, 11.9 mmol, 2 eq.) and SiO_2 (cat.) were charged in a 500 mL round bottom flask to which 150 mL of toluene and a few drops of glacial acetic acid were added. A condenser was then adapted, and the reaction mixture set to reflux for 4 days open to air. The crude of the reaction was filtered while hot and the filtrate washed with diethyl ether (2 x 50 mL). Removal of volatiles *in vacuo* yielded a dark brown powder which was recrystallised from acetone, affording the desired product as bright yellow needles. (2.75 g, 79%). ^1H NMR (400 MHz, $CDCl_3$) δ 13.02 (s, 1H, N*H*), 8.94 (s, 2H, (N=C*H*)), 8.40 (d, 2H, *J*= 1.7 Hz, H4 + H5), 8.17 (d, *J*= 8.9 Hz, 2H, Naph *H*8'), 7.86 (d, 2H, *J*= 1.8 Hz, H2 + H7), 7.56 (d, 2H, *J*= 8.2 Hz, Naph *H*4'), 7.46-7.41 (m, 4H, Naph *H*3' and *H*5'), 7.17 (dd, 2H, *J*= 7.2 and 1.0 Hz, Naph *H*2'), 6.95 (ddd, 2H, *J*= 8.1, 6.9 and 1.0 Hz Naph *H*6'), 6.38 (ddd, 2H, *J*= 8.1, 6.9 and 1.0 Hz Naph *H*7'), 1.59 (s, 18H, C(C*H*₃)₃). $^{13}C\{^1H\}$ NMR (100 MHz, $CDCl_3$) δ 160.97 (N=*C*H), 149.59 (N-*C*1'), 142.51 (C3 + C6), 137.14 (C8a + C9a), 133.64 (quatern-Naph *C*4a'), 128.75 (quatern-Naph *C*8a'), 127.80 (C2 + C7), 126.72 (Naph *C*5'), 125.69 (Naph *C*4' and *C*6'), 125.58 (Naph *C*3'), 124.97 (Naph *C*7'), 123.80 (Naph *C*8'), 123.70 (C1 + C8), 120.21 (C4 + C5), 119.56 (4a + 4b), 112.62 (Naph *C*2'), 34.98 (*C*(CH₃)₃), 32.23 (C(*C*H₃)₃). HRMS/ESI- *m/z*: [M+H] calculated 586.3217, found 586.3215 formula $C_{42}H_{40}N_3$. Anal. Calcd for $C_{42}H_{39}N_3$: C 85.82, H 7.03, N 7.15; Found C 83.07, H 6.61, N 6.98. UV/vis (THF, c = 1.0 x 10-5 mol dm^{-3}): λ_{max}/nm (ε x 10^4 / $dm^3mol^{-1}cm^{-1}$) 393 (2.78). IR *v*/cm^{-1} (ATR): 3349 (N*H*), 3044, 2952, 2901, 1591 (N=CH), 1567, 1482.

Synthesis of 1,8-dinaphthylimino-3,6-di(^{t}Butyl)-9-lithium-carbazole(THF) (**2**):

In a Schlenk, **1** (150 mg, 0.25 mmol) and ^{t}BuLi (17 mg, 0.25 mmol) were charged. The flask was cooled down to −78 °C and THF (30 mL) was slowly added, affording a bright orange mixture. The resulting solution was allowed to reach room temperature slowly and left stirring for an additional hour. Volatiles were removed under vacuum affording a bright orange solid (75 mg, 45%). Crystals suitable for XRD were grown from a concentrated hexane solution at room temperature. ^{1}H NMR (300 MHz, C$_6$D$_6$) δ 8.81 (d, 1.9H, J= 1.5 Hz, H4 + H5), 8.63 (s, 2H, (N=C*H*)), 8.28 (d, 2H, J= 8.4 Hz, Naph *H*5'), 7.78 (d, 2H, J= 1.9 Hz, H2 + H7), 7.58 (d, 2H, J= 8.2 Hz, Naph *H*8'), 7.42 (d, 2H, J= 8.3 Hz, Naph *H*4'), 7.23-7.18 (m, 4H, Naph *H*3' and *H*7'), 6.91 (ddd, 2H, J= 8.2, 6.9 and 1.2 Hz, Naph *H*6'), 6.85 (dd, 2H, J= 7.2 and 1 Hz, Naph *H*2'), 1.60 (s, 18H, C(C*H*$_3$)$_3$). ^{7}Li{^{1}H} NMR (117 MHz, C$_6$D$_6$/C$_4$D$_8$O) δ 3.02, 2.31 (s). ^{13}C{^{1}H} NMR (100 MHz, C$_6$D$_6$) δ 167.81 (N=*C*H), 152.27 (N-*C*1'), 151.04 (C3 + C6), 138.26 (C8a + C9a), 134.77 (C4a + C4b), 129.65 (C2 + C7), 129.17 (quatern-Naph *C*8a'), 128.27 (quatern-Naph *C*4a'), 127.92 (Naph *C*8'), 127.0 (Naph *C*6'), 126.71 (Naph *C*3'), 126.41 (Naph *C*7'), 123.46 (Naph *C*4'), 122.78 (Naph *C*5'), 120.76 (C4 + C5), 120.35 (C1 + C8), 115.94 (Naph *C*2'), 35.19 (*C*(CH$_3$)$_3$), 32.92 (C(*C*H$_3$)$_3$). HRMS/EI m/z: [M-C$_4$H$_8$O]$^+$ calculated 590.3211, found 590.3215 formula C$_{42}$H$_{38}$N$_3$Li. UV/vis (THF, c = 1.0 x 10^{-5} mol dm^{-3}): λ_{max}/nm (ε x10^4 / dm^{3}mol^{-1}cm^{-1}) 396 (2.48). IR v/cm^{-1} (Nujol): 2930, 2726, 1629, 1594, 1304.

Synthesis of 1,8-dinaphthylimino-3,6-di(^{t}Butyl)-9-sodium-carbazole(THF) (**3**):

In a Schlenk, **1** (200 mg, 0.34 mmol) and NaH (16.4 mg, 0.68 mmol, 2 eq.) were charged. The flask was cooled down to 0 °C and THF (30 mL) was slowly added. The resulting suspension was stirred at 0 °C for 30 min. After this time, the vessel was allowed to reach room temperature and stirred overnight. The resulting dark red suspension was filtered to remove unreacted NaH and the volatiles were removed under vacuum yielding an orange powder (82 mg, 36%). Crystals suitable for XRD were grown from a concentrated hexane solution at room temperature. ^{1}H NMR (400 MHz, C$_6$D$_6$) δ 8.82 (d, 2H, J = 1.9 Hz, H4 + H5), 8.64 (s, 2H, (N=C*H*)), 8.12 (d, 2H, J = 8.3 Hz, Naph *H*5'), 7.76 (d, 2H, J = 1.9 Hz, H2 + H7), 7.59 (d, 2H, J = 8.1 Hz, Naph *H*8'), 7.44 (d, 2H, J = 8.3 Hz, Naph *H*4') 7.24 (t, 2H, J= 7.51 Hz, Naph *H*3'), 7.21 (ddd, 2H, J = 14.87, 8.17 and 1.09 Hz, Naph *H*7'), 7.13 (ddd, 2H, J = 15.17, 8.05 and 1.13 Hz, Naph *H*6'), 6.86 (d, 2H, J = 6.7 Hz, Naph *H*2'), 1.60 (s, 18H, C(C*H*$_3$)$_3$). ^{13}C{^{1}H} NMR (100 MHz, C$_6$D$_6$) δ 169.09 (N=*C*H), 152.17 (N-*C*1'), 151.46 (C3 + C6), 137.0 (C8a + C9a), 134.36 (quatern-Naph *C*8a'), 131.48 (C2 + C7), 129.02 (quatern-Naph *C*4a'), 128.42 (Naph *C*8'), 127.94 (C4a + C4b), 126.80 (Naph *C*6'), 126.60 (Naph *C*3'), 126.49 (Naph *C*7'), 124.84

(Naph $C4'$), 122.78 (Naph $C5'$), 121.98 (C4 + C5), 120.74 (C1 + C8), 115.27 (Naph $C2'$), 34.69 ($C(CH_3)_3$), 32.52 (C(CH_3)$_3$). HRMS/EI m/z: [M-C_4H_8O]$^+$ calculated 607.2958, found 607.2955 formula $C_{42}H_{38}N_3Na$. UV/vis (THF, c = 1.0 x 10^{-5} mol dm^{-3}): λ_{max}/nm (ε x10^4 / dm^{3}mol^{-1}cm^{-1}) 395 (7.63). IR v/cm^{-1} (Nujol): 3052, 2726, 1625, 1599, 1561.

Synthesis of 1,8-dinaphthylimino-3,6-di(^{t}Butyl)-9-potassium-carbazole (**4**):

In a Schlenk, the ligand, **1** (200 mg, 0.34 mmol) and KH (27 mg, 0.68 mmol, 2 eq.) were charged. The flask was cooled down to 0 °C and THF (30 mL) was slowly added. The resulting suspension was allowed to reach room temperature and left stirring for additional 3 hours. The resulting dark red suspension was filtered to remove unreacted hydride. Volatiles were removed under vacuum yielding the product as a dark orange-red powder (110 mg, 42%). Crystals suitable for XRD were grown from a concentrated hexane solution at room temperature. ^{1}H NMR (400 MHz, C_6D_6) δ 8.86 (d, 2H, J= 1.07 Hz, H4 + H5), 8.63 (s, 2H, (N=CH)), 8.27-8.25 (m, 2H, Naph $H5'$), 7.80 (d, 2H, J= 1.1 Hz, H2 + H7), 7.67-7.65 (m, 2H, Naph $H8'$), 7.52 (d, 2H, J= 8.2 Hz, Naph $H4'$), 7.33 (d, 2H, J= 7.4 Hz, Naph $H3'$), 7.30-7.28 (m, 4H, Naph $H6'$ + $H7'$), 6.84 (d, 2H, J= 7.1 Hz, Naph $H2'$), 1.60 (s, 18H, C(CH_3)$_3$). ^{13}C{^{1}H} NMR (100 MHz, C_6D_6) δ 168.28 (N=CH), 152.30 (N-$C1'$), 152.20 (C3 + C6), 136.38 (C8a + C9a), 134.66 (quatern-Naph $C8a'$), 132.14 (C2+C7), 128.32 (Naph $C8'$), 128.83 (quatern-Naph $C4a'$), 127.39 (C4a+ C4b), 126.88 (Naph $C3'$), 126.85 (Naph $C6'$), 126.78 (Naph $C7'$), 124.74 (Naph $C4'$), 123.55 (Naph $C5'$), 121.71 (C4 + C5), 121.51 (C1 + C8), 114.67 (Naph $C2'$), 34.63 ($C(CH_3)_3$), 32.55 (C(CH_3)$_3$). HRMS/ASAP m/z: [M+H]$^+$ calculated 624.2781, found 624.2797 formula $C_{42}H_{39}N_3K$, UV/vis (THF, c = 5.0 x 10^{-6} mol dm^{-3}): λ_{max}/nm (ε x10^4 / dm^{3}mol^{-1}cm^{-1}) 389 (9.73). IR v/cm^{-1} (Nujol): 3052, 2726, 1623, 1603, 1571.

Typical dehydrogenation procedure using catalytic amounts of the group 1 salts and Me$_2$NH·BH$_3$:

In a glovebox, **3** (5.76 mg, 8.48 x10^{-3} mmol) and Me$_2$NH·BH$_3$ (10 mg, 0.16 mmol, 20 eq.) were dissolved in 0.6 mL of either C_6D_6 or THF (with a C_6D_6 insert) and transferred to a Young's tap modified borosilicate glass NMR tube. The resulting NMR sample was transferred to an oil bath set up to the desired temperature (Table 1) and monitored until the resonances attributed to the starting material disappeared (^{11}B NMR spectroscopy) or when no significant reaction progress was observed.

<u>Open system experiments:</u>

In a glovebox, **3** (5.76 mg, 8.48 x10^{-3} mmol) and Me$_2$NH·BH$_3$ (10 mg, 0.16 mmol, 20 eq.) were dissolved in 0.6 mL of toluene and transferred to a Young's tap modified borosilicate glass NMR tube containing a magnetic stirrer (Note: the magnetic stirrer was removed following the catalysis, in a glovebox, prior to NMR determinations). The resulting NMR sample was adapted to a system constituted by a glass adapter, a three-way tap (attached to a Schlenk line) and an inverted burette filled with paraffin oil (see below). An oil bath was warmed up to 70 °C and after careful deoxygenation of the whole system, the NMR sample was warmed up. The three-way tap was then opened to the bubbler, allowing the concomitant liberation of H$_2$ to be measured over time by displacement of the paraffin oil. The volume of H$_2$ determined using this methodology, closely correlates with similar conversion determined by ^{11}B NMR spectroscopy (Table 1, Entry 5).

<u>Scale-Up:</u>

In a glovebox, **3** (57.6 mg, 0.0848 mmol) and Me$_2$NH·BH$_3$ (100 mg, 1.69 mmol, 20 eq.) were dissolved in 6 mL of toluene and transferred to a Schlenk tube containing a magnetic stirrer. The resulting bright orange solution was adapted under N$_2$ flow, to a system constituted by a glass adapter, a three-way tap (attached to a Schlenk line) and an inverted burette filled with paraffin oil (see below). An oil bath was warmed up to 70 °C and after careful deoxygenation of the whole system, the system was warmed up. The three-way tap was then opened to the bubbler, allowing the concomitant liberation of H$_2$ to be measured over time by displacement of the paraffin oil. The volume of H$_2$ determined using this methodology, closely correlates with similar conversion determined by ^{11}B NMR spectroscopy.
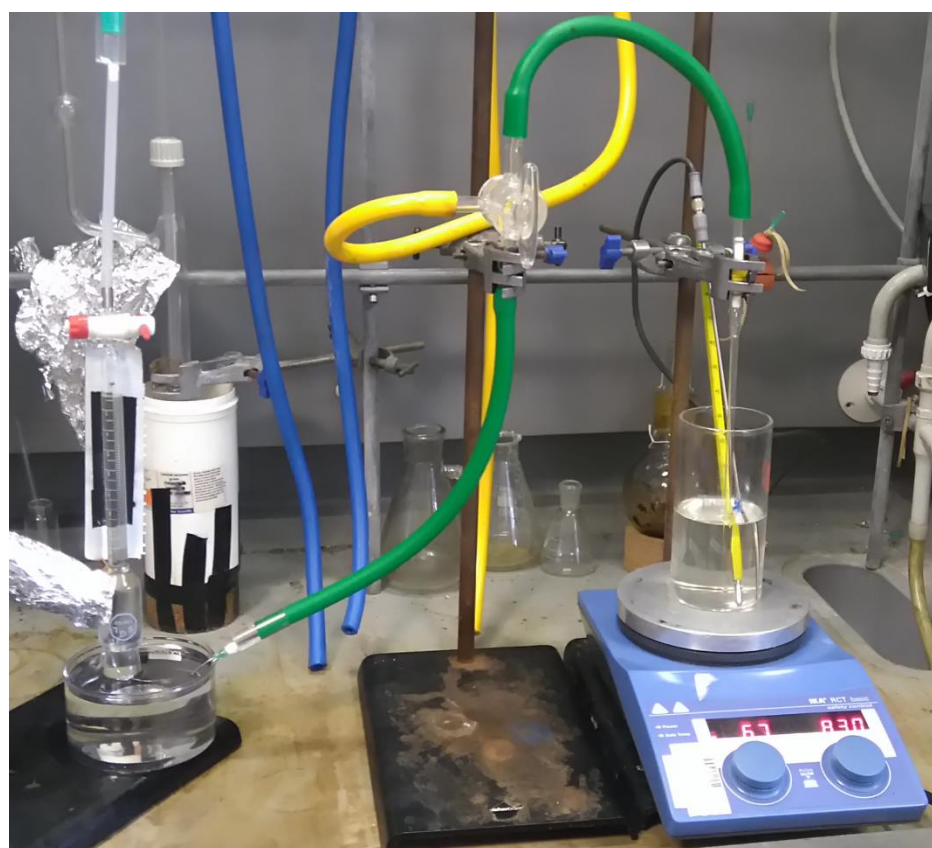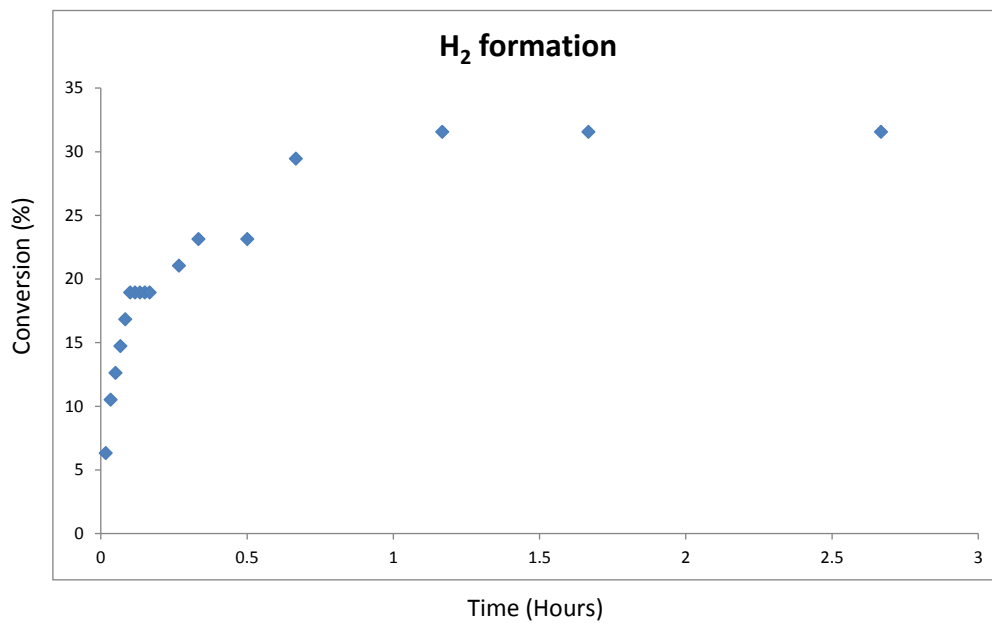
Figure S1. Graph representing the formation of H₂ in an open system (top) and set-up (bottom).

Nitrogen based solvents + Metal complexes

$$M\left[Me_2N\overset{H_2}{B}\underset{Me_2}{N}BH_3\right] + Nu \rightleftharpoons M\left[Me_2N\overset{H_2}{B}NMe_2\right] + Nu\cdot BH_3 \rightleftharpoons MBH_4 + Nu + Me_2N\overset{H}{B}NMe_2$$

M= Li, Na *or* K   Nu= Py, MeCN or Morpholine

Nitrogen based solvents in absence of metal

$$Me_2HN\cdot BH_3 + Nu \rightleftharpoons Nu\cdot BH_3 + HNMe_2$$

Nu= Py, MeCN or Morpholine
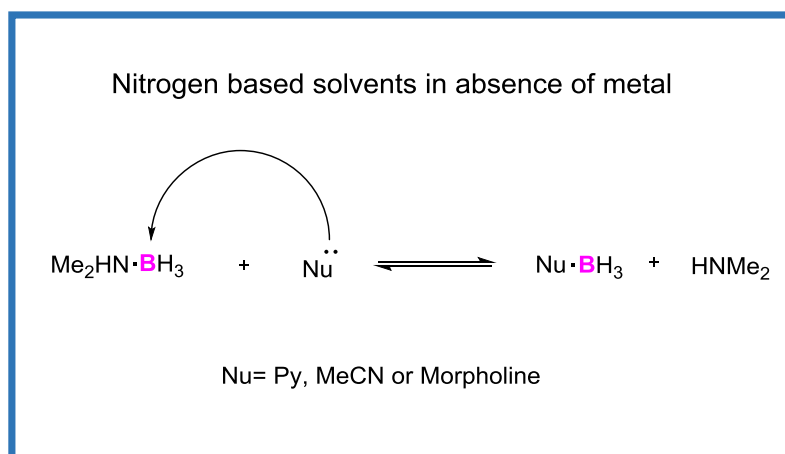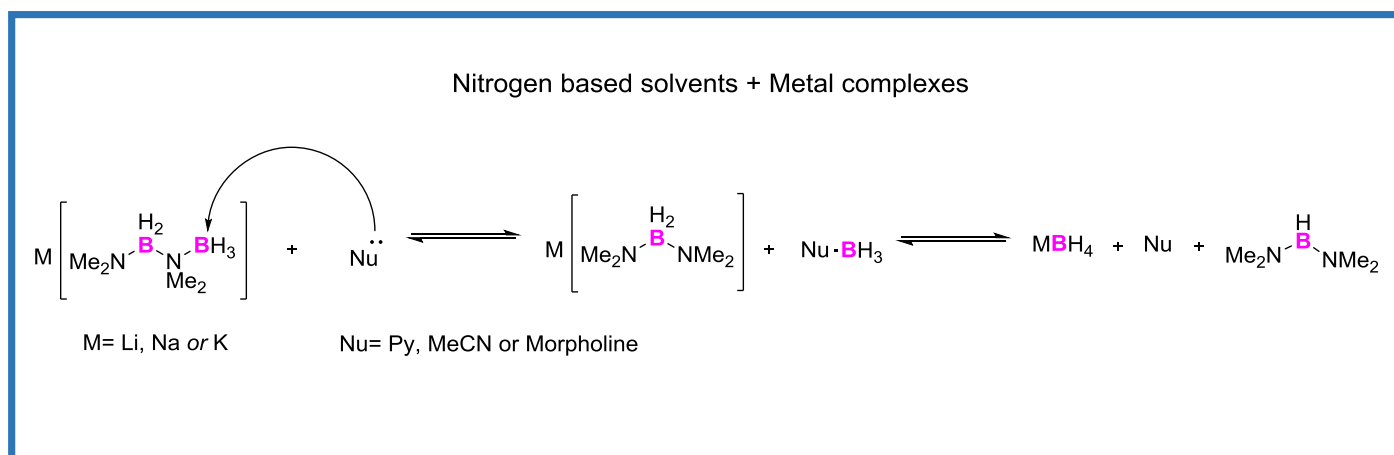
Scheme S1. Proposed mechanistic pathway for the formation of **7**.

Selected NMR spectra
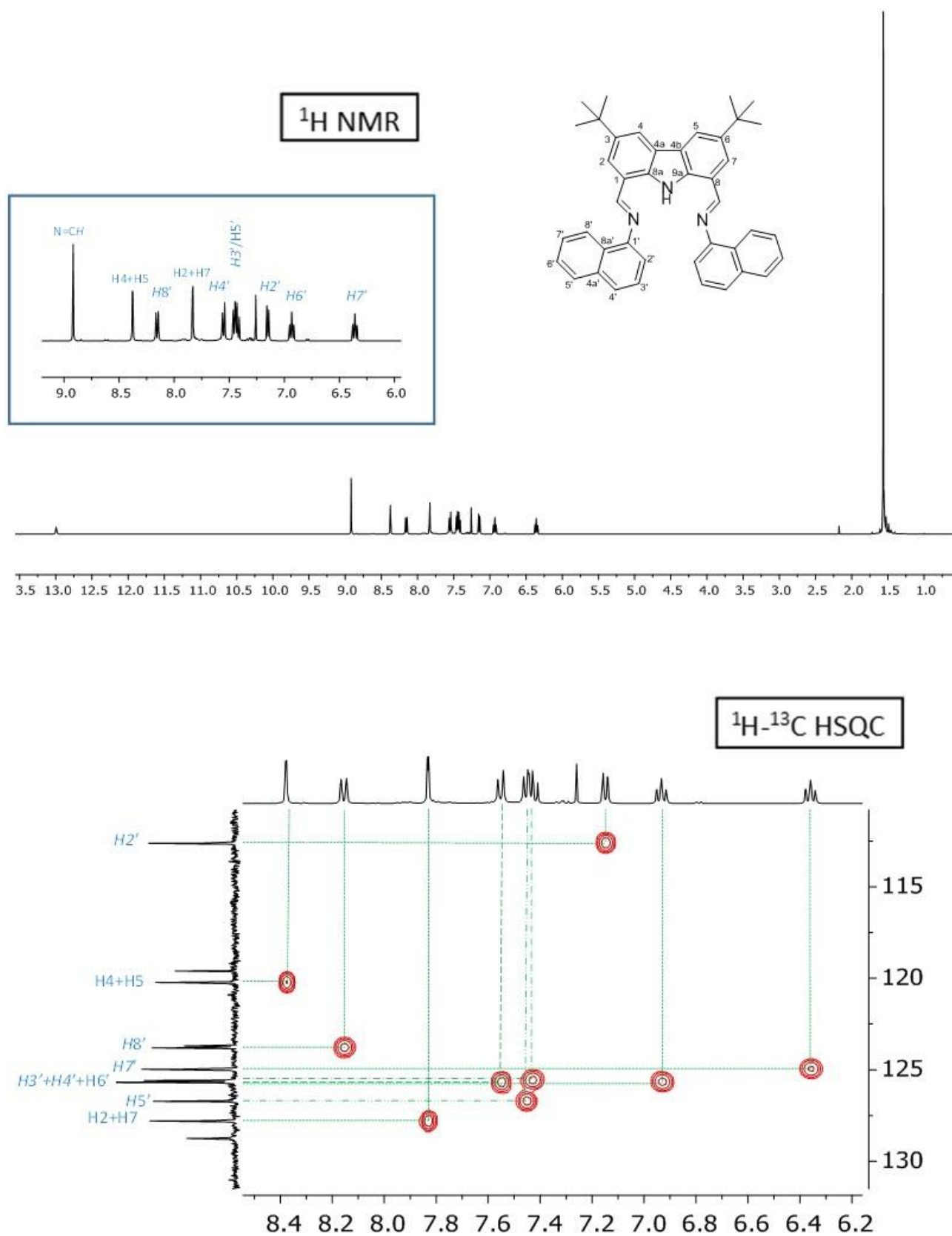
Figure S2. [1]H and selected region ^{1}H,^{13}C-HSQC NMR spectra of **1** in CDCl₃.
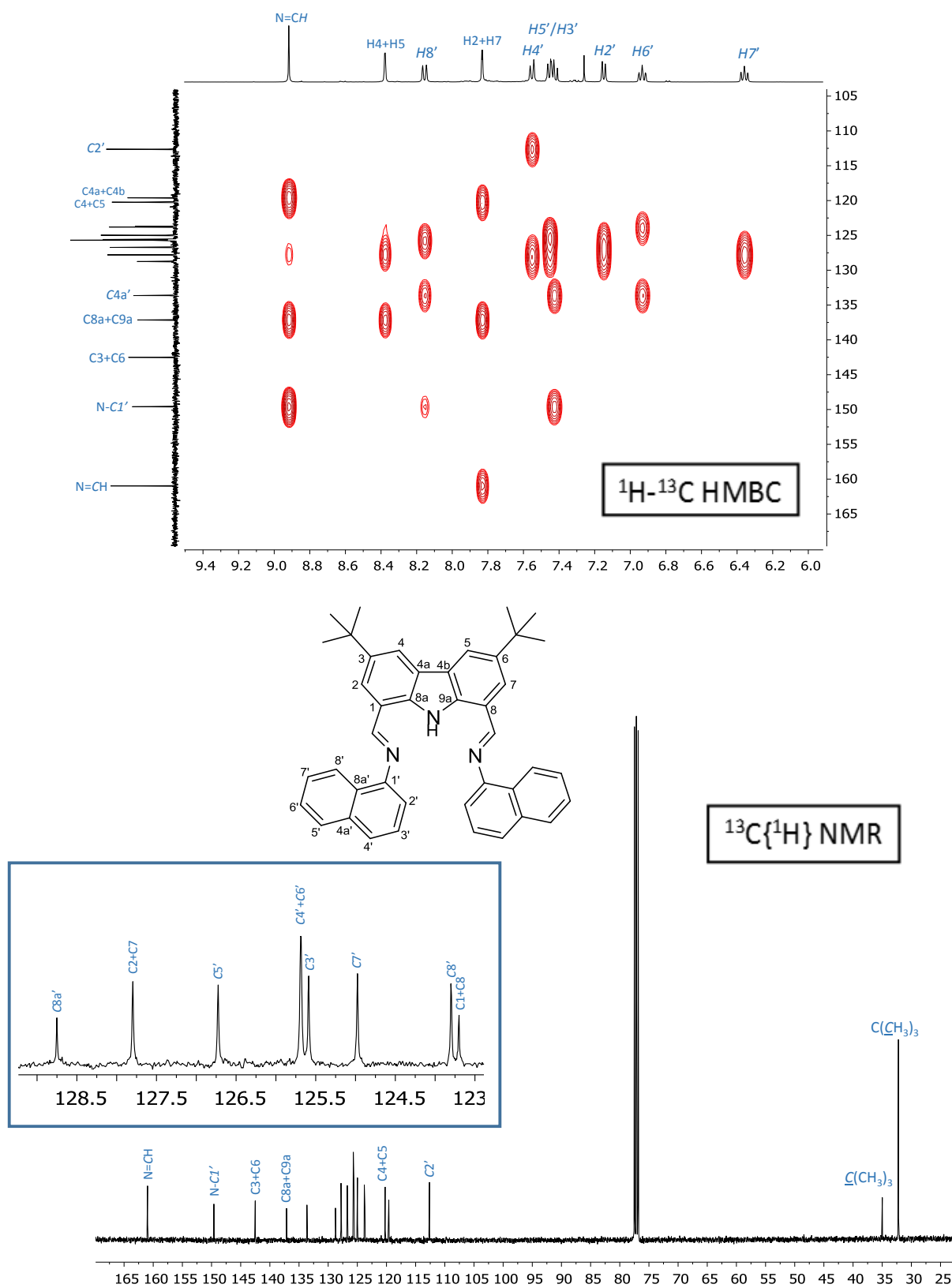
Figure S3. $^{13}C\{^1H\}$ and selected region of the $^1H,^{13}C$-HMBC NMR spectra complex of **1** in CDCl₃.
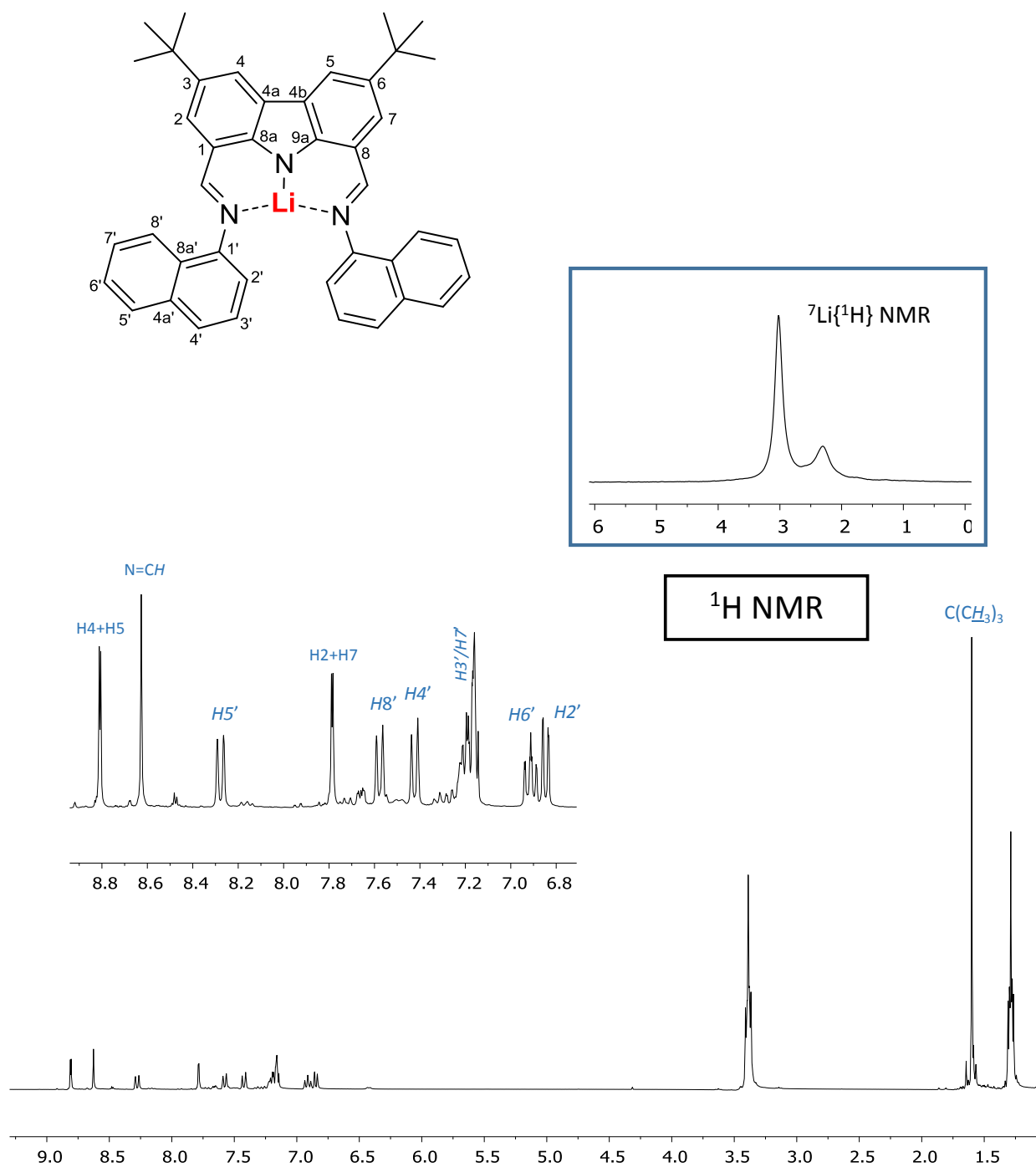
Figure S4. ^{1}H and ^{7}Li{^{1}H} NMR (framed in blue) spectra complex of **2** in C_6D_6.
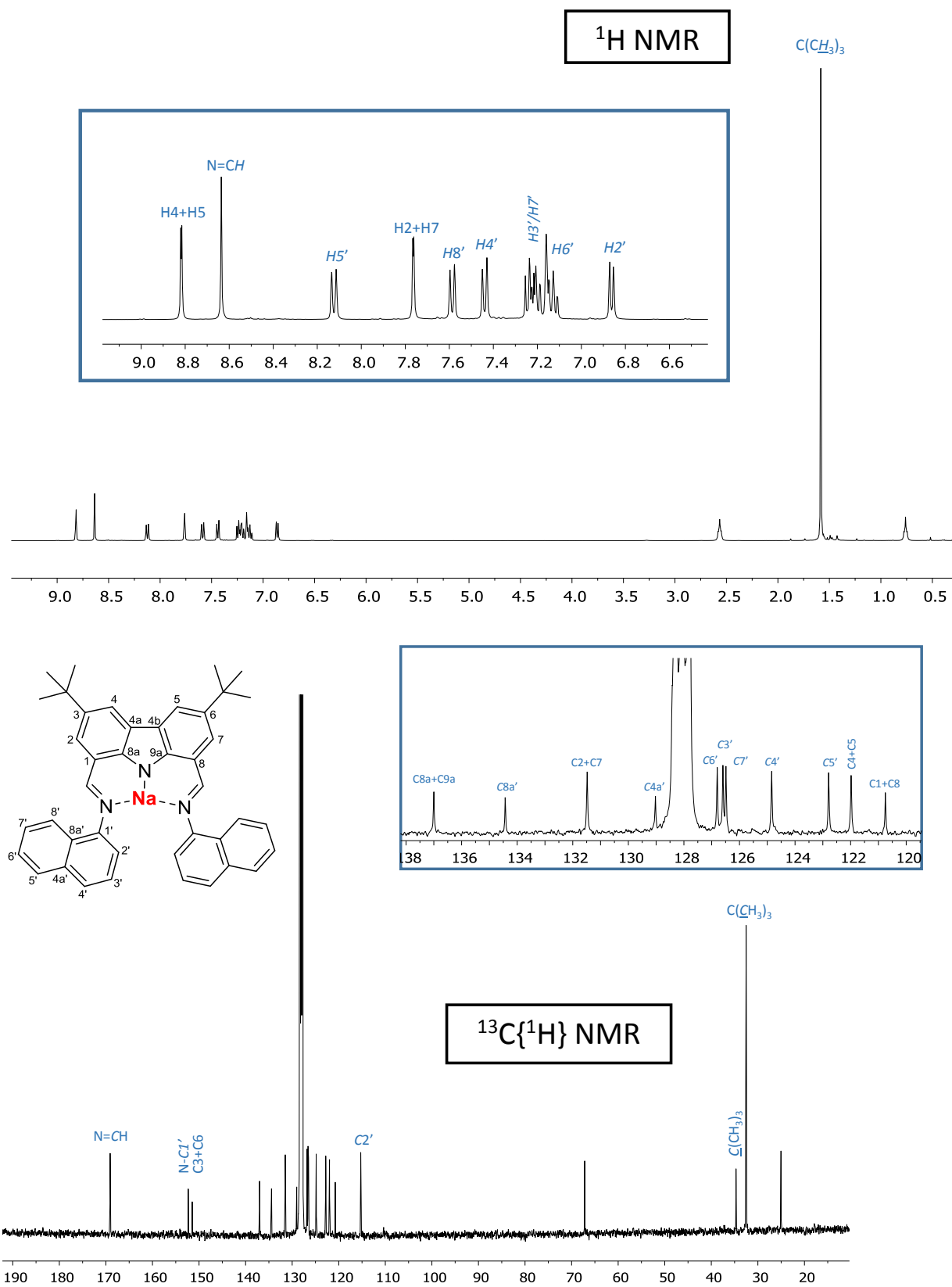
Figure S5. ^{1}H and $^{13}C\{^{1}H\}$ NMR spectra of complex **3** in C_6D_6.
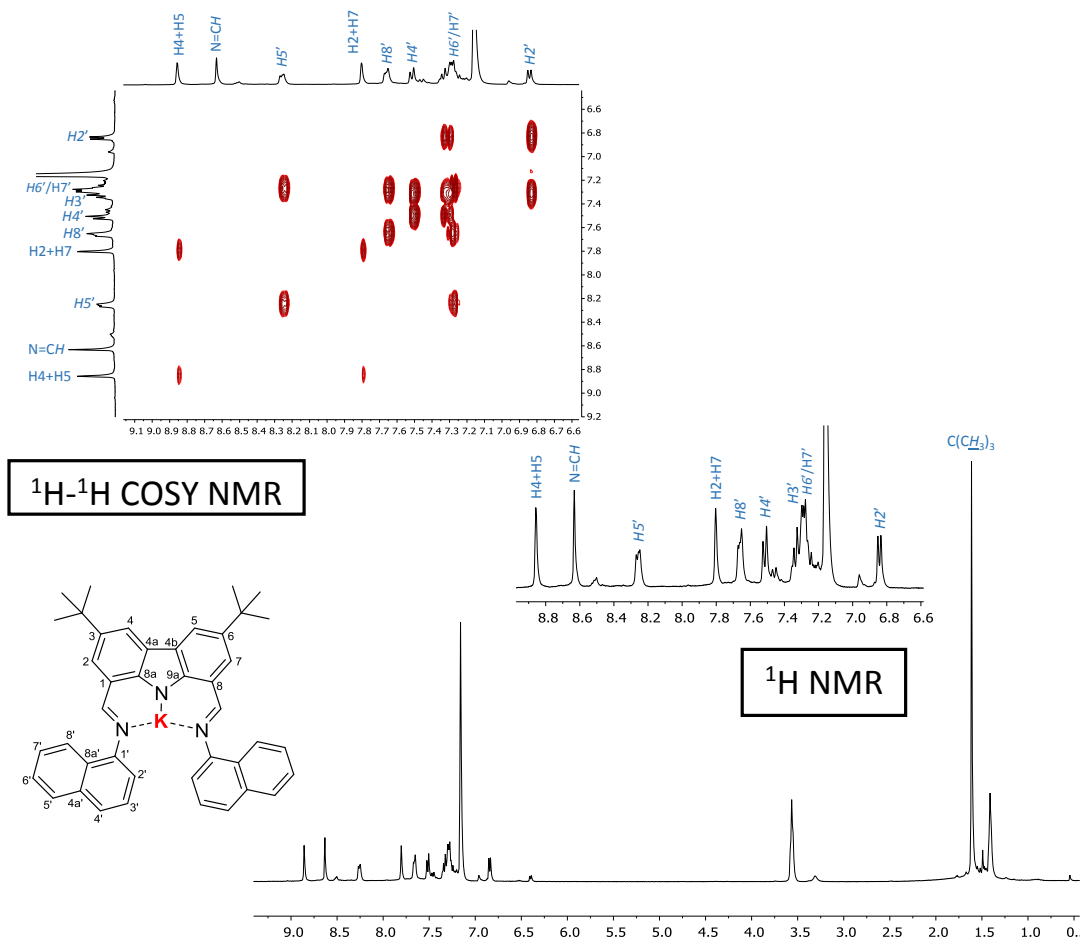
Figure S6. ^{1}H and selected region of the ^{1}H,^{1}H-COSY NMR spectra of complex **4** in C$_6$D$_6$.
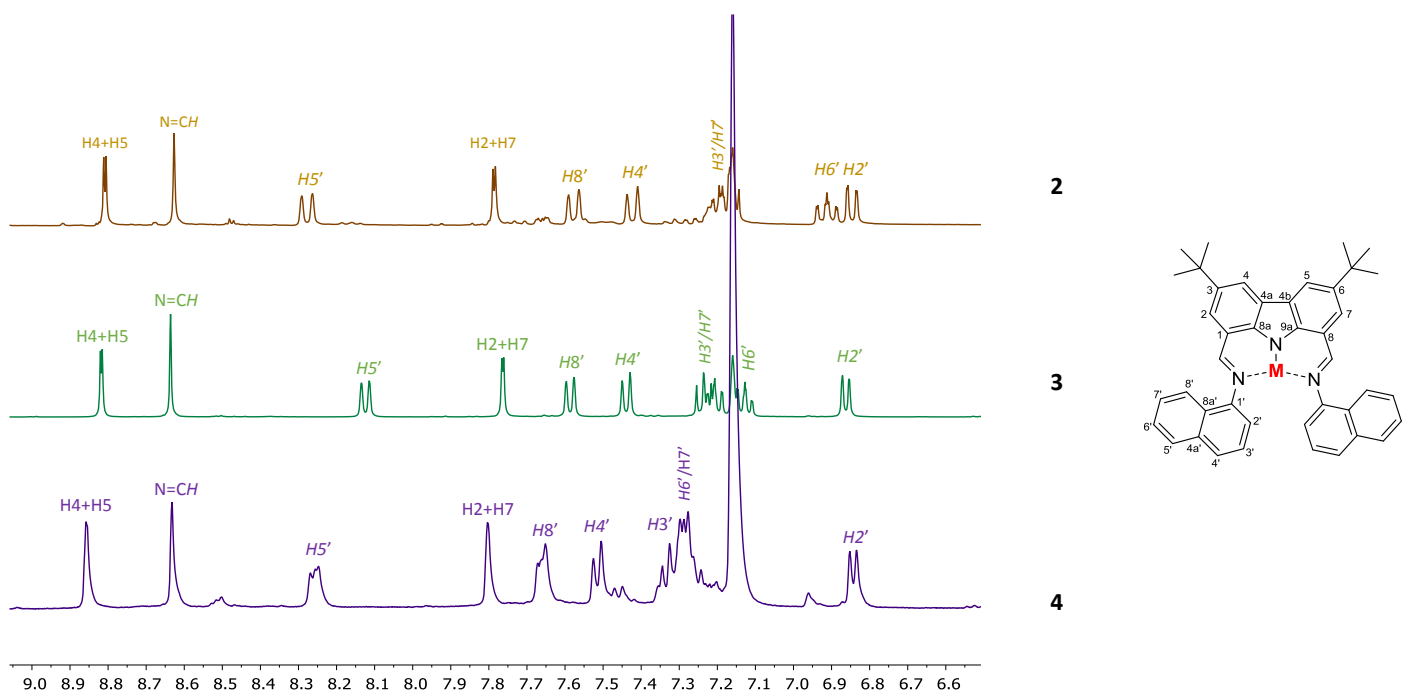
Figure S7. Selected region of the ^{1}H NMR spectra of complex **2** (yellow), **3** (green) and **4** (purple) in C$_6$D$_6$.
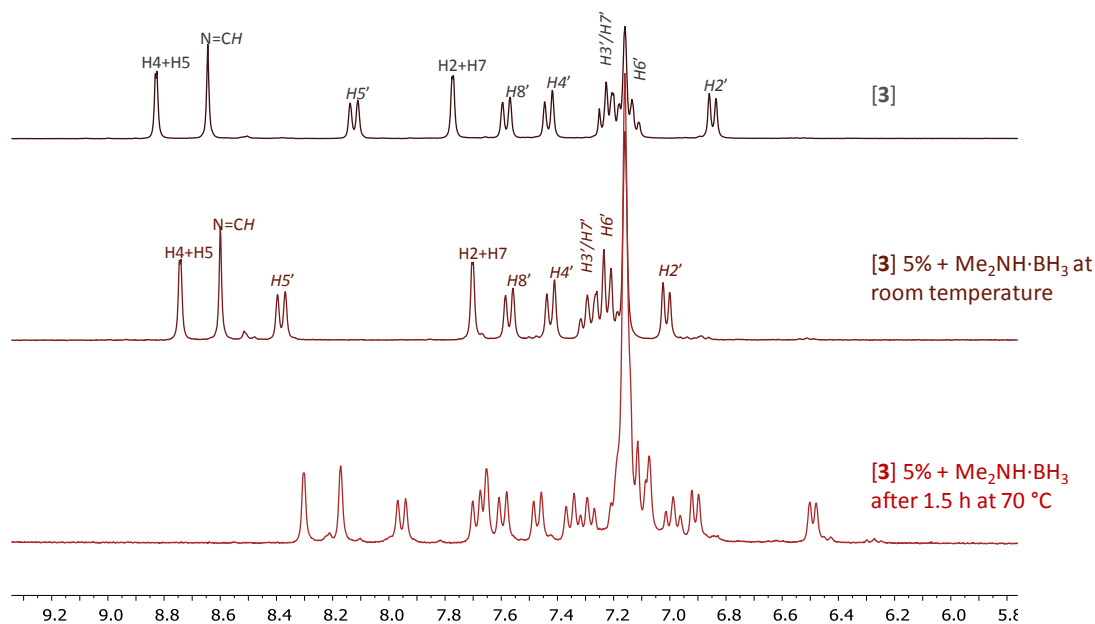
Figure S8. Selected region of the ^{1}H NMR spectra of complex **3** (above), after addition of Me$_2$NH·BH$_3$ at rt (middle) and after heating at 70 °C (below) in C$_6$D$_6$.
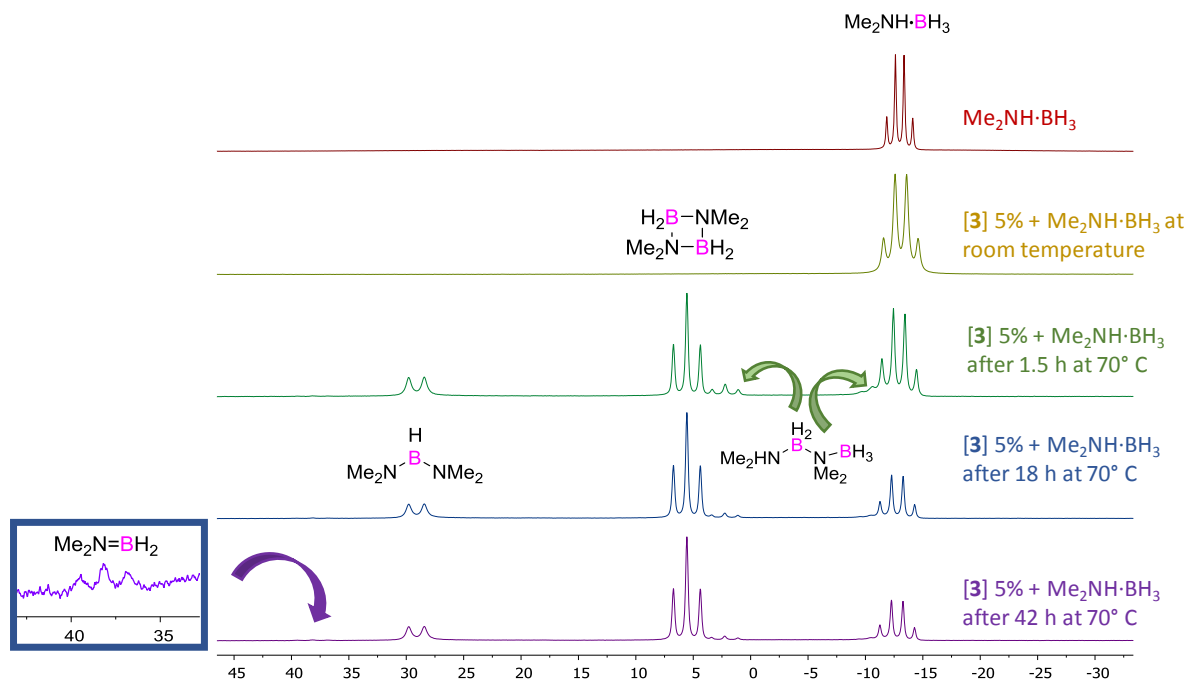
Figure S9. Monitoring by ^{11}B NMR spectroscopy of the reaction between complex **3** (5 mol%) and Me$_2$NH·BH$_3$ in C$_6$D$_6$.
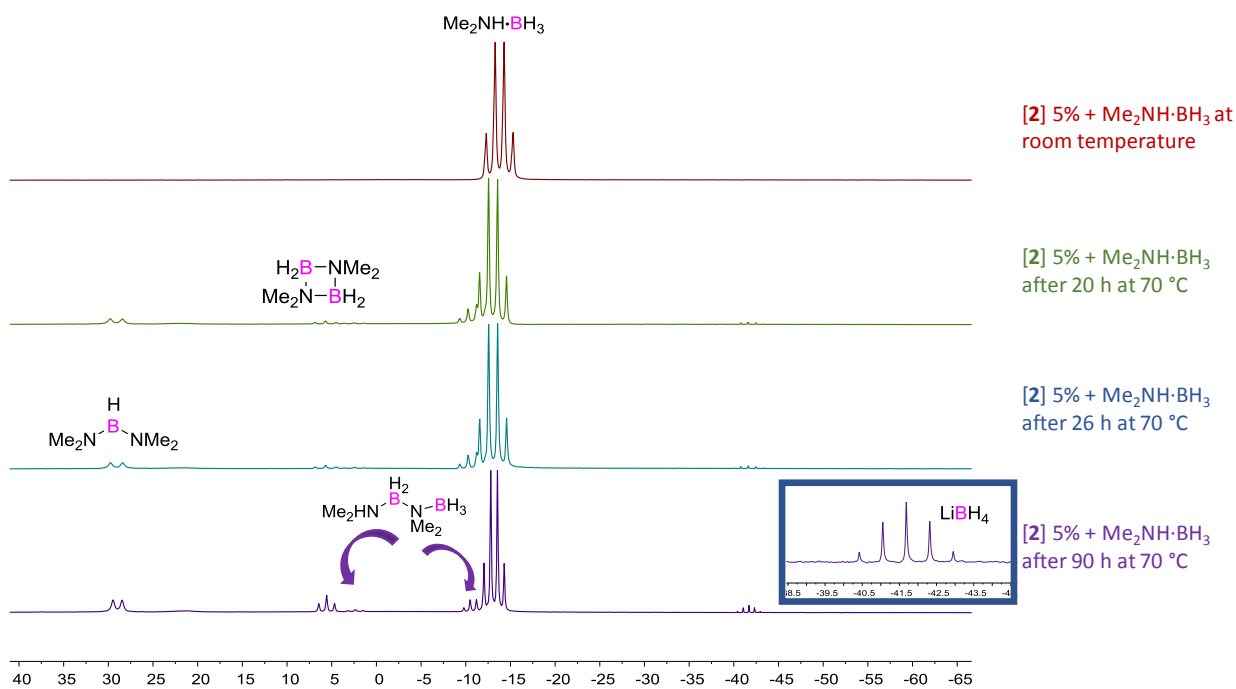
Figure S10. Monitoring by ^{11}B NMR spectroscopy of the reaction between complex **2** (5 mol%) and Me$_2$NH·BH$_3$ in C$_6$D$_6$.
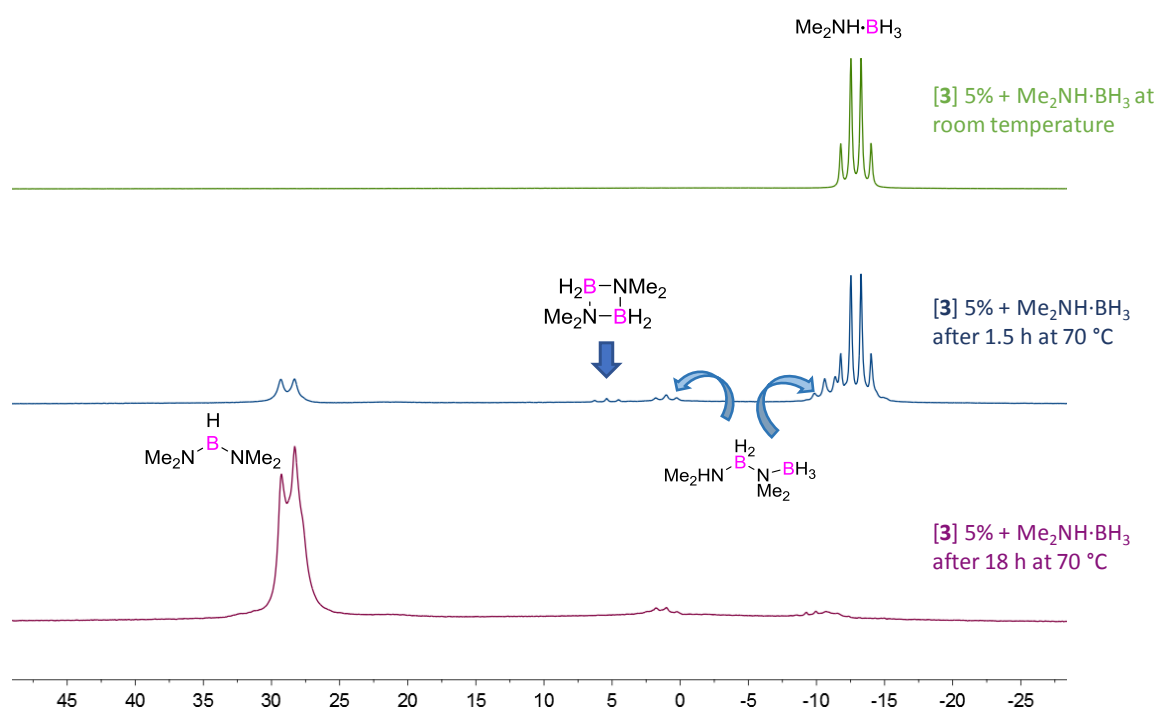
Figure S11. Monitoring by ^{11}B NMR spectroscopy of the reaction between complex **3** (5 mol%) and Me$_2$NH·BH$_3$ in pyridine.
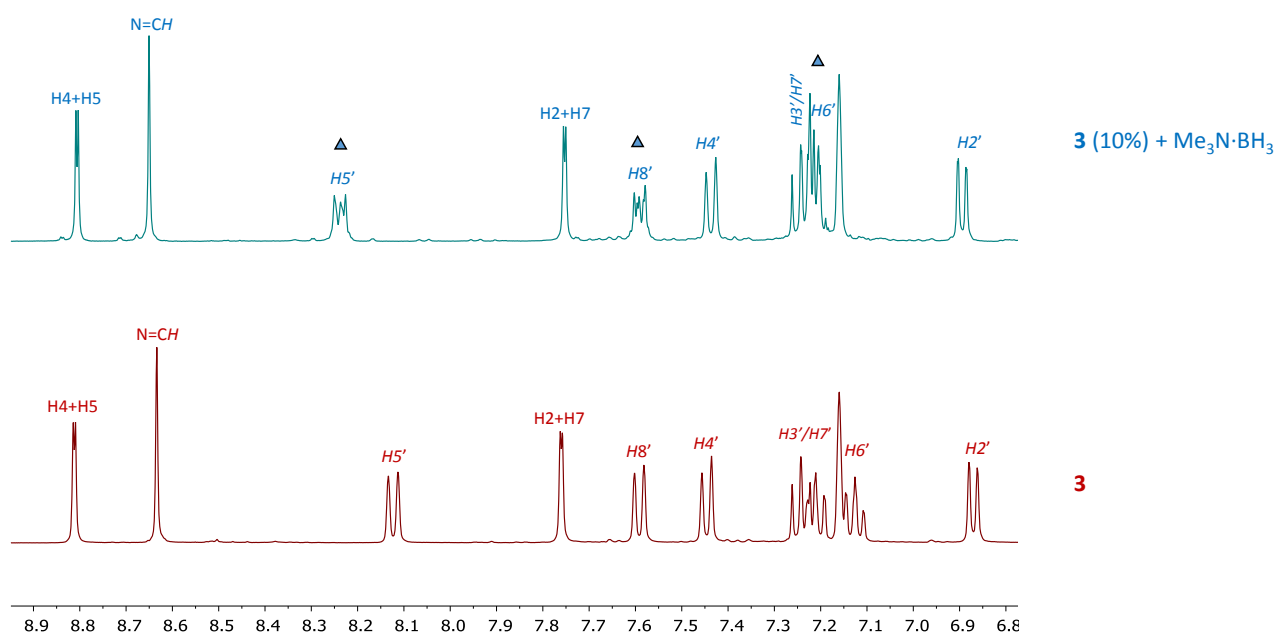
Figure S12. Monitoring by ^{1}H NMR spectroscopy of the reaction between complex **3** (10 mol%) and Me$_3$N·BH$_3$ in C$_6$D$_6$.
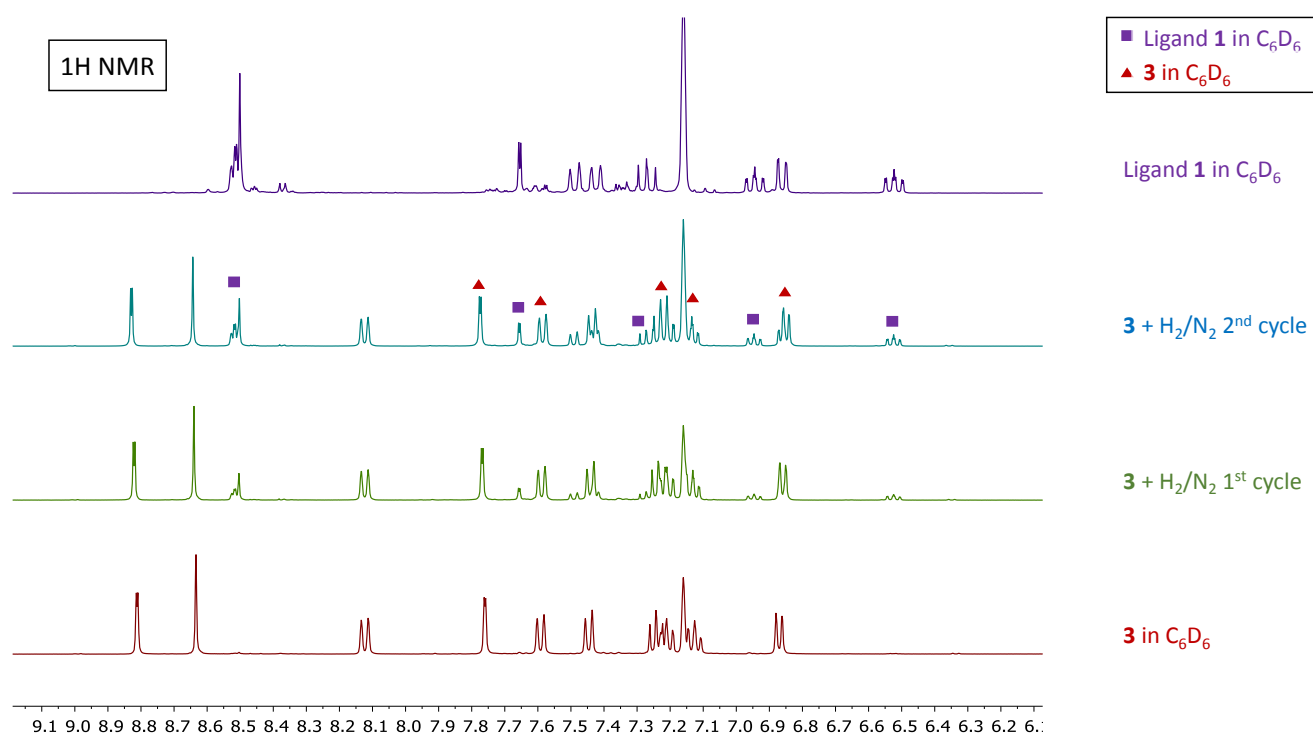
Figure S13. Monitoring by ^{1}H NMR spectroscopy of the reaction between complex **3** and H$_2$(g) in C$_6$D$_6$.

Table S1. ^{11}B NMR chemical shifts for relevant compounds observed in $Me_2NH \cdot BH_3$ dehydrocoupling reactions.

Compound	^{11}B NMR Chemical Shift (δ)	Reference
$Me_2NH \cdot BH_3$	-12.3 (q)	*Chem. Eur. J.*, **2011**, *17*, 4099-4103.
$Me_3N \cdot BH_3$	-7.70 (q)	*Chem. Ber.* **1966**, *99*, 1049-1067.
$Me_2N=BH_2$	37.9 (t)	*J. Organomet. Chem.*, **2016**, *821*, 154-162.
$HB(NMe_2)_2$	29 (d)	*Chem. Eur. J.*, **2010**, *16*, 8508-8515.
$B(NMe_2)_3$	-21 (br)	*J. Organomet. Chem.*, **2016**, *821*, 154-162.
$[Me_2N-BH_2]_2$	5.5 (t)	*J. Am. Chem. Soc.*, **2003**, *125*, 9424-9434.
$Me_2HN-BH_2-NMe_2-BH_3$	2.3 (t), -13.1 (q)	*Chem. Eur. J.*, **2011**, *17*, 4099-4103.
$Li[Me_2NBH_2NMe_2BH_3]$	3.5 (t), -14.7 (q)	*Dalton Trans.*, **2015**, *44*, 12078-12081.
$Na[Me_2NBH_2NMe_2BH_3]$	1.9 (t), -14.7 (q)	*Dalton Trans.*, **2015**, *44*, 12078-12081.
$K[NMe_2BH_2NMe_2BH_3]$	2.6 (t), -12.3 (q)	*Dalton Trans.*, **2015**, *44*, 12078-12081.
$Na[H_3BNMe_2BH_2NMe_2BH_3]$	28 (br)	*Inorg. Chem.*, **2013**, *52*, 10690-10697.
$Na[H_3B-NMe_2-BH_3]$	29.7 (br)	*Eur. J. Inorg. Chem.*, **1999**, 1373-1379.
Oligo/polymers	26-36 (br)	*J. Am. Chem. Soc.*, **2003**, *125*, 9424-9434.
$LiBH_4$	-41.5 (quint)	*J. Phys. Chem.* C., **2014**, 6596-6603.
$NaBH_4$	-42.4 (quint)	*Eur. J. Phys Chem.*, **1959**, *63*, 1533-1535.
KBH_4	-38.7 (quint)	*J. Phys. Chem.* C., **2014**, 6596-6603.
Pyridine$\cdot BH_3$	-11.6 (q)	*RSC Adv.*, **2014**, *4*, 26207–26210.
Morpholine$\cdot BH_3$	-14.8 (q)	*RSC Adv.*, **2014**, *4*, 26207–26210.

DOSY

Table S2. Diffusion coefficients obtained from DOSY NMR spectroscopy (21 °C).

Substrate	Diffusion Coefficient	Hydrodynamic Radius
3[a]	$5.34 \times 10^{-10} m^2/s$	$5.49 \times 10^{-10} m$
3 + $Me_2NH \cdot BH_3$ at room temperature[a]	$5.45 \times 10^{-10} m^2/s$	$5.38 \times 10^{-10} m$
3 + $Me_2NH \cdot BH_3$ after heating at 70 °C for 0.5 hour[a]	$6.28 \times 10^{-10} m^2/s$	$4.67 \times 10^{-10} m$
3 + $Me_2NH \cdot BH_3$ after heating at 70 °C for 0.5 hour[b]	$5.89 \times 10^{-10} m^2/s$	$4.98 \times 10^{-10} m$

[a]Ratio **3**:$Me_2NH \cdot BH_3$ 1:1, Concentration [0.017M]; [b]Ratio **3**: $Me_2NH \cdot BH_3$ 1:20, Concentration [0.014M]
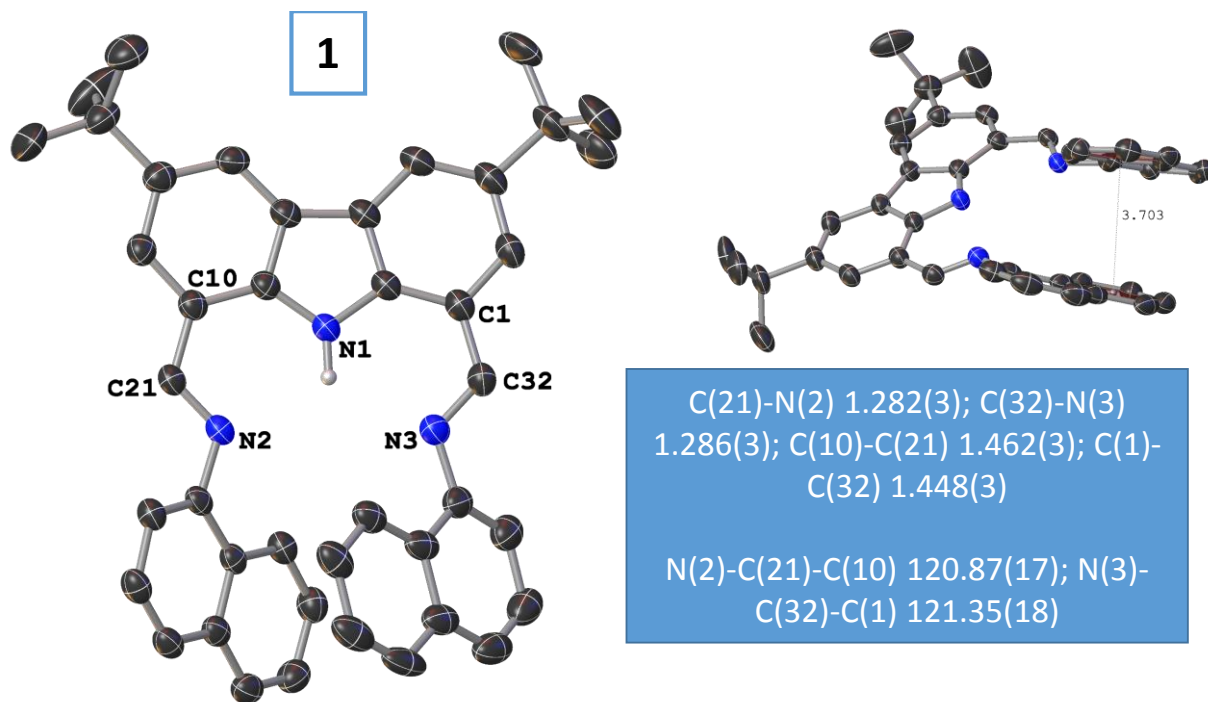
Figure S14. Molecular structure of **1** with displacement ellipsoids set at the 50% probability level. Hydrogen atoms have been omitted for clarity.
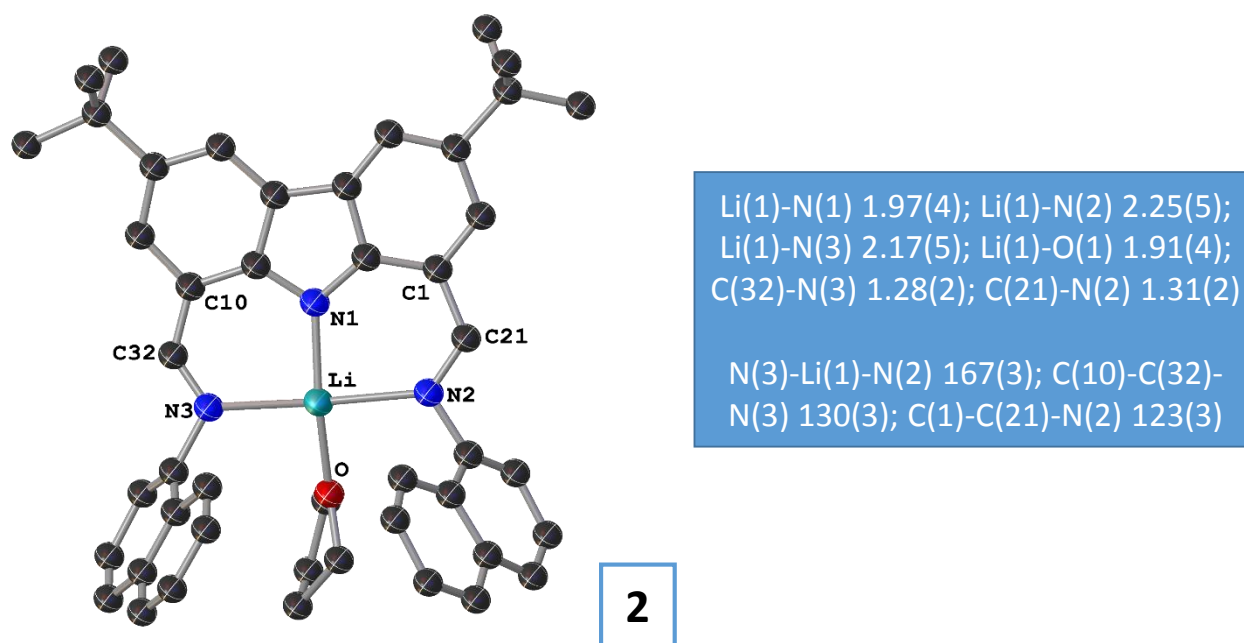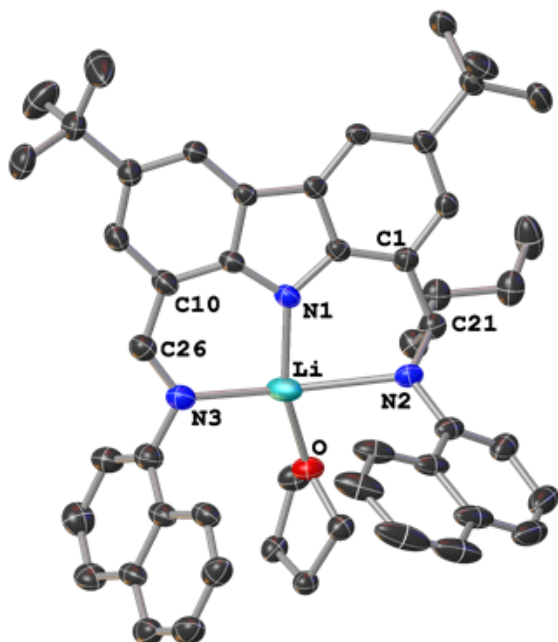
C(21)-N(2) 1.282(3); C(32)-N(3) 1.286(3); C(10)-C(21) 1.462(3); C(1)-C(32) 1.448(3)

N(2)-C(21)-C(10) 120.87(17); N(3)-C(32)-C(1) 121.35(18)

Figure S15. Molecular structure of **2** with displacement ellipsoids set at the 50% probability level. Hydrogen atoms have been omitted for clarity.

Li(1)-N(1) 1.97(4); Li(1)-N(2) 2.25(5); Li(1)-N(3) 2.17(5); Li(1)-O(1) 1.91(4); C(32)-N(3) 1.28(2); C(21)-N(2) 1.31(2)

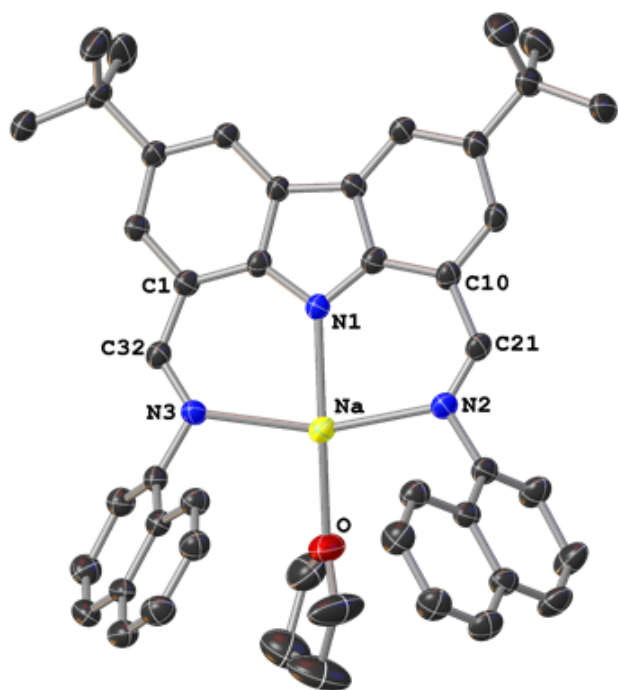N(3)-Li(1)-N(2) 167(3); C(10)-C(32)-N(3) 130(3); C(1)-C(21)-N(2) 123(3)

2a

Li(1)-N(1) 1.933(3); Li(1)-N(2) 2.644(4); Li(1)-N(3) 2.117(4); Li(1)-O(1) 1.914(3); C(26)-N(3) 1.292(2); C(21)-N(2) 1.4895(19)

N(3)-Li(1)-N(2) 160.24(15); C(10)-C(26)-N(3) 125.68(16); C(1)-C(21)-N(2) 108.10(12)

Figure S16. Molecular structure of alkylated **2** with displacement ellipsoids set at the 50% probability level. Hydrogen atoms have been omitted for clarity.
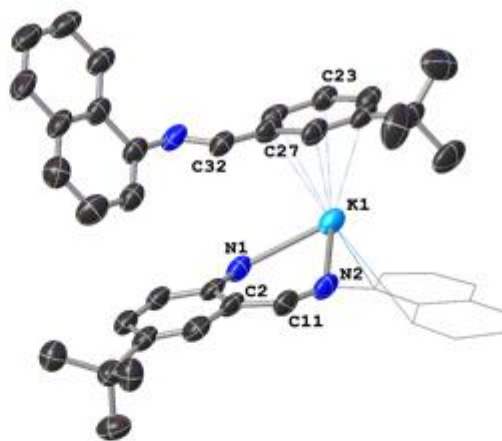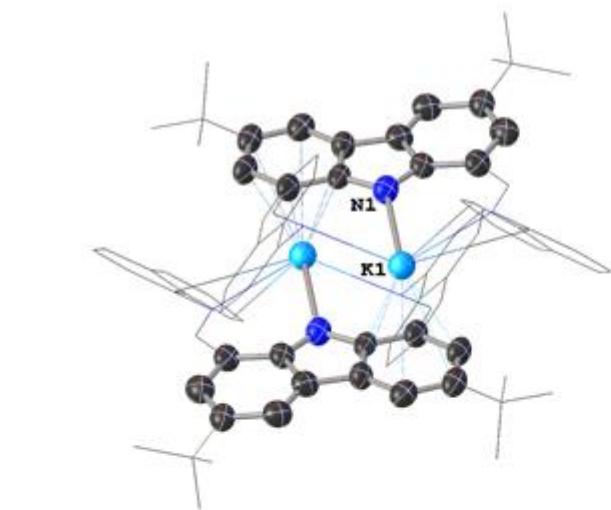

Na(1)-N(1) 2.287(3); Na(1)-N(2) 2.398 (3); Na(1)-N(3) 2.408(3); C(21)-N(2) 1.275(4); C(32)-N(3) 1.296(4); Na(1)-O(1) 2.294(3)
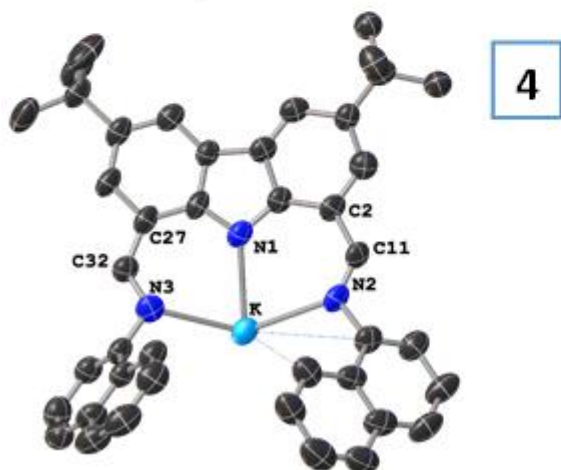
N(1)-Na(1)-O(1) 164.62(15); N(3)-Na(1)-N(2) 158.09(12); N(2)-C(21)-C(10) 126.7(3); N(3)-C(32)-C(1) 126.0(3)

3

Figure S17. Molecular structure of **3** with displacement ellipsoids set at the 50% probability level. Hydrogen atoms have been omitted for clarity.

K(1)-N(1) 2.680(8); K(1)-N(2) 2.747(8); K(1)-N(3) 2.762(9); C(23)$_{plane}$-K(1) 2.984(9)

N(2)-C(11)-C(2) 127.1(8); N(3)-C(32)-C(27) 127.1(9)

Figure S18. Molecular structure of **4** with displacement ellipsoids set at the 50% probability level. Hydrogen atoms have been omitted for clarity.

C(6)-N(3) 1.466(8); N(3)-B(5) 1.547(10); N(3)-B(6) 1.569(10); N(3)-C(5) 1.495(10)

C(5)-N(3)-C(6) 107.7(9); C(6)-N(3)-B(6) 109.0(8); B(5)-N(3)-B(6) 112.2(10); C(6)-N(3)-B(5) 109.4(10)
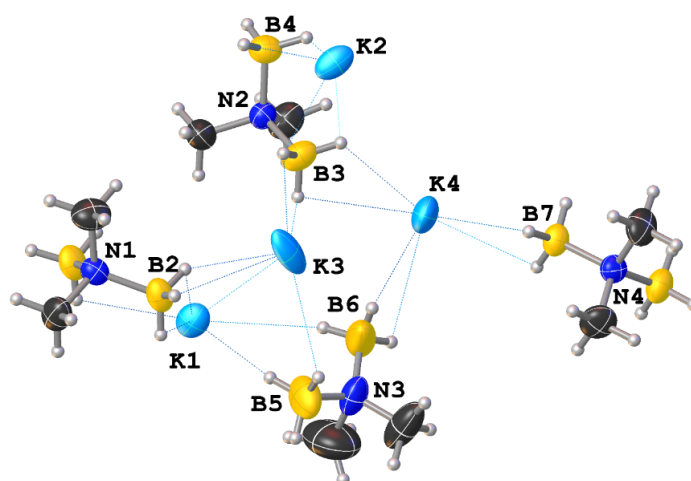
Asymmetric unit of **8a**

Figure S19. Molecular structure of **8a** with displacement ellipsoids set at the 50% probability level. Hydrogen atoms have been omitted for clarity.

Crystallographic Methods

Under a flow of N_2, crystals suitable for X-ray diffraction were quickly removed from the crystallisation vessel and covered with "fomblin" (YR-1800 perfluoropolyether oil). A suitable crystal was then mounted on a polymer-tipped MicroMount™ and cooled rapidly to 120K in a stream of cold N_2 using an Oxford Cryosystems open flow cryostat.[1] Single crystal X-ray diffraction data were collected either using an Agilent SuperNova diffractometer, Atlas CCD area detector (mirror-monochromated Cu-$K\alpha$ radiation source; $\lambda = 1.54184$ Å or graphite-monochromated Mo-Kα radiation source; $\lambda = 0.7103$ Å; ω scans), an Agilent SuperNovaII diffractometer, Atlas S2 CCD area detector, an Agilent SuperNovaII diffractometer Titan S2 CCD area detector (mirror monochromated Cu-$K\alpha$ radiation source; $\lambda = 1.54184$ Å; ω scans) or a Rigaku MM007 rotating anode X-ray source. Absorption corrections were applied using an analytical numerical method (CrysAlis Pro).[2] All non-H atoms were located using direct methods[3] and difference Fourier syntheses. Hydrogen atoms were placed and refined using a geometric riding model. All fully occupied non-H atoms were refined with anisotropic displacement parameters, unless otherwise specified. Crystal structures were solved and refined using the Olex2 software package.[4] Programs used include CrysAlisPro[5] (control of Supernova, data integration and absorption correction), SHELXL[6] (structure refinement), SHELXS[7] (structure solution), SHELXT[8] (structure solution), OLEX2[4a] (molecular graphics). CIF files were checked using checkCIF[9] CCDC 1581977-1581982 contain the supplementary data for **1, 2, 2a, 3, 4** and **8a**. These data can be obtained free of charge from The Cambridge Crystallographic Data Centre *via* www.ccdc.cam.ac.uk/data_request/cif.

Crystal data for 1,8-dinaphthylimino-3,6-di(^tButyl)–9H-carbazole (1): CCDC 1581977

$C_{42}H_{39}N_3$ ($M = 585.76$ g/mol): monoclinic, space group $P2_1/c$ (no. 14), $a = 28.8139(16)$ Å, $b = 8.5704(4)$ Å, $c = 13.5865(7)$ Å, $\beta = 102.756(5)°$, $V = 3272.3(3)$ Å^3, $Z = 4$, $T = 120(2)$ K, μ(CuKα) = 0.528 mm^{-1}, $Dcalc = 1.189$ g/cm^3, 24982 reflections measured (9.442° ≤ 2Θ ≤ 148.76°), 6597 unique ($R_{int} = 0.0651$, $R_{sigma} = 0.0477$) which were used in all calculations. The final R_1 was 0.0565 (I > 2σ(I)) and wR_2 was 0.1609 (all data).

Crystal data for 1,8-dinaphthylimino-3,6-di(^tButyl)–9-lithium-carbazole(THF) (2): CCDC 1581978

$C_{46}H_{46}LiN_3O$ ($M = 663.80$ g/mol): triclinic, space group P-1 (no. 2), $a = 12.023(8)$ Å, $b = 12.802(10)$ Å, $c = 13.927(7)$ Å, $a = 66.18(6)°$, $\beta = 76.98(5)°$, $\gamma = 73.37(6)°$, $V = 1864(2)$ Å^3, $Z = 2$, $T = 120(2)$ K, μ(CuKα) = 0.536 mm^{-1}, $Dcalc = 1.182$ g/cm^3, 1794 reflections measured (6.992° ≤ 2Θ ≤ 61.838°), 1150 unique ($R_{int} = 0.0884$, $R_{sigma} = 0.2702$) which were used in all calculations. The final R_1 was 0.0967 (I > 2σ(I)) and wR_2 was 0.2415 (all data).

Crystal data for 2a: CCDC 1581979

$C_{50}H_{55}LiN_3$ ($M = 720.91$ g/mol): monoclinic, space group $P2_1/n$ (no. 14), $a = 13.65773(16)$ Å, $b = 21.7068(3)$ Å, $c = 14.23975(17)$ Å, $\beta = 105.0737(12)°$, $V = 4076.34(8)$ Å^3, $Z = 4$, $T = 120(2)$ K,

μ(CuKα) = 0.526 mm^{-1}, $Dcalc$ = 1.175 g/cm^3, 46635 reflections measured (7.61° ≤ 2Θ ≤ 147.678°), 8151 unique (R_{int} = 0.0352, R$_{sigma}$ = 0.0202) which were used in all calculations. The final R_1 was 0.0479 (I > 2σ(I)) and wR_2 was 0.1304 (all data).

Crystal data for 1,8-dinaphthylimino-3,6-di(^{t}Butyl)-9-sodium-carbazole(THF) (**3**): **CCDC 1581980**

C$_{52}$H$_{60}$N$_3$NaO (M =766.02 g/mol): triclinic, space group P-1 (no. 2), a = 12.1323(9) Å, b = 13.7056(11) Å, c = 14.2286(11) Å, a = 90.659(7)°, β = 106.001(7)°, γ = 103.336(7)°, V = 2205.8(3) Å^3, Z = 2, T = 120(2) K, μ(CuKα) = 0.605 mm^{-1}, $Dcalc$ = 1.153 g/cm^3, 16325 reflections measured (7.816° ≤ 2Θ ≤ 149.182°), 8049 unique (R_{int} = 0.0593, R$_{sigma}$ = 0.0767) which were used in all calculations. The final R_1 was 0.0808 (I > 2σ(I)) and wR_2 was 0.2593 (all data).

Crystal data for 1,8-dinaphthylimino-3,6-di(^{t}Butyl)-9-potassium-carbazole (**4**): **CCDC 1581981**

C$_{84}$H$_{76}$K$_2$N$_6$ (M =1247.70 g/mol): triclinic, space group P-1 (no. 2), a = 11.670(3) Å, b = 11.773(2) Å, c = 12.928(4) Å, a = 80.79(2)°, β = 85.14(2)°, γ = 78.098(18)°, V = 1713.1(8) Å^3, Z = 1, T = 120.02(10) K, μ(CuKα) = 1.602 mm^{-1}, $Dcalc$ = 1.209 g/cm^3, 10407 reflections measured (7.754° ≤ 2Θ ≤ 133.182°), 5952 unique (R_{int} = 0.1123, R$_{sigma}$ = 0.1518) which were used in all calculations. The final R_1 was 0.1335 (I > 2σ(I)) and wR_2 was 0.3859 (all data).

Crystal data for [H$_3$B-NMe$_2$-BH$_3$]K (**8a**): **CCDC 1581982**

C$_2$H$_{12}$B$_2$KN (M =110.85 g/mol): monoclinic, space group P2$_1$/n (no. 14), a = 9.6343(3) Å, b = 22.8460(8) Å, c = 13.1641(4) Å, β = 91.402(3)°, V = 2896.63(17) Å^3, Z = 16, T = 120(2) K, μ(CuKα) = 5.437 mm^{-1}, $Dcalc$ = 1.017 g/cm^3, 16081 reflections measured (7.74° ≤ 2Θ ≤ 147.702°), 5696 unique (R_{int} = 0.0558, R$_{sigma}$ = 0.0528) which were used in all calculations. The final R_1 was 0.0867 (I > 2σ(I)) and wR_2 was 0.2395 (all data).

References

[1]   J. Cosier, A. M. Glazer, *J. Appl. Crystallogr.* **1986**, *19*, 105-107.
[2]   A. Technologies, **2013**.
[3]   G. M. Sheldrick, *Acta Crystallogr. Sect. A: Found. Crystallogr.* **2008**, *64*, 112-122.
[4]   a) O. V. Dolomanov, L. J. Bourhis, R. J. Gildea, J. A. K. Howard, H. Puschmann, *J. Appl. Crystallogr.* **2009**, *42*, 339-341; b) O. V. Dolomanov, A. J. Blake, N. R. Champness, M. Schroder, *J. Appl. Crystallogr.* 2003, *36*, 1283-1284.
[5]   CrysAlisPRO Oxford Diffraction/Agilent Technologies UK Ltd Yarnton England.
[6]   G. M. Sheldrick, *Acta Crystallogr. Sect. C Struct. Chem.* **2015**, *71*, 3-8.
[7]   G. M. Sheldrick, *Acta Crystallogr. Sect. A Found. Crystallogr.* **2008**, *64*, 112-122.
[8]   G. M. Sheldrick, *Acta Crystallogr. Sect. A Found. Crystallogr.* **2015**, *71*, 3-8.
[9]   http://checkcif.iucr.org